

Received xxx, 2022, accepted xxx, 2022.

Digital Object Identifier xxx

# Probabilistic Meta-Conv1D Driving Energy Prediction for Mobile Robots in Unstructured Terrains

MARCO VISCA<sup>1</sup>, ROGER POWELL<sup>2</sup>, YANG GAO<sup>3</sup>, AND SABER FALLAH<sup>1</sup>

<sup>1</sup>Connected and Autonomous Vehicles Lab (CAV Lab), University of Surrey, Guildford, GU2 7XH, UK. Email: {m.visca, s.fallah}@surrey.ac.uk

<sup>2</sup>Cybernetics Group, Remote Applications in Challenging Environments, UK Atomic Energy Authority, Culham Science Centre, OX14 3DB.

<sup>3</sup>Space Technology for Autonomous and Robotic Laboratory (STAR LAB), University of Surrey, Guildford, GU2 7XH, UK. Email: yang.gao@surrey.ac.uk

Corresponding author: Saber Fallah (e-mail: s.fallah@surrey.ac.uk).

This work has been carried out within the framework of the EUROfusion Consortium, funded by the European Union via the Euratom Research and Training Programme (Grant Agreement No 101052200 — EUROfusion). Views and opinions expressed are however those of the author(s) only and do not necessarily reflect those of the European Union or the European Commission. Neither the European Union nor the European Commission can be held responsible for them.

**ABSTRACT** Driving energy consumption plays an important role in the navigation of autonomous mobile robots in off-road scenarios. However, the accuracy of the driving energy predictions is often affected by a high degree of uncertainty due to unknown and constantly varying terrain properties, and the complex wheel-terrain interaction in unstructured terrains. In this paper, we propose a probabilistic deep meta-learning approach to model the existing uncertainty in the driving energy consumption and efficiently adapt the probabilistic predictions based on a small number of local measurements. Our method expands upon an existing deterministic deep-meta learning model that, in contrast, only provided single-point energy estimates. The performance of our method is compared against the deterministic approach in a 3D-body dynamic simulator over several typologies of deformable terrains and unstructured geometries. In this way, we provide evidence of the benefit of the proposed method to enhance the predictions with informative probabilistic considerations, which can be crucial to the safety of mobile robots traversing challenging, unstructured environments.

**INDEX TERMS** Autonomous mobile robots, deep learning, energy-aware path planning, meta-learning, probabilistic neural networks

## I. INTRODUCTION

AUTONOMOUS mobile robots (AMRs) can be applied in a variety of tasks requiring them to traverse rough, unstructured terrains, such as search and rescue activities, nuclear plant inspections, agriculture, and planetary exploration. In these scenarios, the driving energy consumption (i.e., the energy expended by the AMR traction system) plays a crucial role in the success and efficiency of the mission [1] [2] [3]. Indeed, AMRs in off-road scenarios have often limited energy supplies and their activities involve moving for long distances. Therefore, an accurate estimation of the AMR driving energy consumption is critical to minimize the time spent recharging, thereby ensuring longer periods of continuous operations.

In off-road scenarios, the driving energy consumption is a complex function of (1) the terramechanical properties of the terrain (i.e., its mechanical characteristics and its response

to vehicular loading and shear stress) and (2) the geometry of the terrain [4]. Particularly, in natural environments, several types of terrains with different characteristics may be encountered, ranging from sand, mud, rocks, and a multitude of intra-classes. However, the terramechanical properties of a terrain are often *a priori* unknown, can constantly change, and are challenging to estimate online [5]–[8].

Regarding the geometry of the terrain, previous works have commonly considered the terrain as a uniformly-sloped surface whose inclination is the only energy-relevant geometric factor [9]–[12]. However, many areas in off-road environments contain complex, unstructured geometries, such as scattered rocks, steps, bumps, and rough terrain. Traversing unstructured geometries can induce complex motion dynamics, uncertain wheel-terrain interactions, and can pose increased challenges to the AMR locomotion and control system [13].

Such complex interplay between varying, unknown terrain properties, unstructured geometries, and its effect on the driving energy consumption, is challenging to model and is affected by considerable uncertainty. However, failing at estimating the driving energy consumption can be detrimental to the safety and efficiency of the AMR. For example, an excessive underestimation of the driving energy may cause the robot to run out of battery and stop ahead of time in a precarious position, causing critical damage to the robot and/or the abortion of the mission. Hence, providing a single-point estimation of driving energy consumption may carry an unacceptable degree of risk, due to the safety-critical nature of many applications in off-road scenarios [14]. In contrast, an approach is desirable that can explicitly reason about the uncertainty in the driving energy prediction.

In a previous work [15], we proposed a meta-learning approach (called Meta-Conv1D), based on deep neural networks, to learn and adapt the driving energy prediction model of an AMR traversing terrains with (1) unknown and varying terramechanical properties and (2) complex unstructured geometries. Specifically, Meta-Conv1D demonstrated the capability to efficiently adapt its energy estimates to unknown terrains based on a small number of local measurements and to analyse the effect of unstructured geometries on the driving energy consumption using Convolutional 1D (Conv1D) neural networks (Section III). However, Meta-Conv1D could only provide single-point energy estimates, while no consideration about the uncertainty of its estimations was provided. In contrast, in many realistic scenarios, the local measurements may not carry enough information to adapt the energy model with high certainty. Moreover, while Meta-Conv1D demonstrated superior performance to previous state-of-the-art methods, its estimates were still affected by increasingly large errors in particularly rough, unstructured environments.

In this paper,

- 1) Our primary contribution is a probabilistic re-framing of the Meta-Conv1D approach. First, we analyze the main factors contributing to the driving energy prediction uncertainty (Section IV). Then, we propose the integration of different probabilistic distribution models within the Meta-Conv1D meta-learning framework (Section V).
- 2) We provide experimental results of our method, in simulation, over several types of natural terrains and unstructured geometries (Section VI) and we compare its performance with the deterministic Meta-Conv1D approach (Section VII).
- 3) We show that our method can correctly model the existing uncertainty in the driving energy prediction caused by (1) the lack of information in the few local measurements used to adapt the energy model (Section VII-A) and (2) the influence of traversing complex, unstructured geometries (Section VII-A and VII-B). Hence, while the standard Meta-Conv1D approach could only provide single-point estimates, often affected by large errors in the more uncertain scenarios, the proposed probabilistic method yields more descriptive uncertainty-aware predictions which can be beneficial to AMRs traversing challenging, off-road environments.

The implementation of our method is made available at [META-CONV1D-PROB](#).

## II. RELATED WORKS

Driving energy prediction methods for AMRs in off-road scenarios typically falls into two categories: (1) physics-based and (2) data-driven. Several works have developed physics-based models that can provide analytical descriptions of the AMR wheel-terrain interaction. Hence, the models can provide accurate estimates of the AMRs contact forces, drawbar pull, as well as driving energy consumption in many natural terrains [16] [17]. However, analytical methods have often demonstrated only approximate modeling of the actual mechanical behavior of many types of terrain [8]. Moreover, they require the knowledge of terrain-dependent parameters that are often *a priori* unknown and difficult to estimate online. Finally, they are often computationally expensive, making them ill-suited for the implementation into fast-paced planning frameworks [18].

To overcome the challenges of physics-based approaches, different methods have been proposed to directly learn energy models from collected data. For example, several methods have categorized the environment as made of a set of distinct terrain classes [19] [20]. Then, terrain classifiers can be adopted to identify the terrain category, while sensors such as LIDAR or stereo vision estimate the terrain geometry [21]. Hence, different data-driven energy models, such as semi-empirical functions [9], [12], [22], look-up tables [10], or neural networks [11] [13] can be adopted to link the terrain geometry to the driving energy consumption for each terrain type. However, these methods cannot account for terrains with unknown properties.

Differently from considering distinct terrain categories, Higa *et al.* [23] proposed a global energy model that analyzes RGB and depth images, based on 2D convolutional neural networks, to determine, at distance, the terramechanical properties and the driving energy consumption of a terrain. However, the prediction of driving energy consumption from images assumes a strong correlation between the terrain's visual appearance and its properties. This is often not true in off-road scenarios as terrains with similar visual appearances may have, in contrast, very different characteristics, thereby requiring different energy costs to be traversed. Moreover, their method was based on the off-line training of a large and representative dataset, while possible online adaptation to unforeseen terrain conditions was not considered.

Given the difficulty of modeling all possible terrain variations in advance, online adaptation algorithms can represent crucial assets. In this context, meta-learning offers a promising approach to enable rapid adaptation based on limited amounts of data [24]. Other works have proposed the use of meta-learning for the online adaptation of robotic platforms [25]–[28]. However, little attention has been given to the problem of driving energy prediction in unstructured terrains. As previously stated, an energy-aware deep meta-learning framework was presented, in [15], called Meta-

Conv1D, to predict, adapt, and plan over terrains with unknown and varying terramechanical properties and complex unstructured geometries. However, Meta-Conv1D could only provide single-point energy estimates, while no consideration about the uncertainty of its estimations was given.

Few works have proposed prediction algorithms for AMRs in unstructured environments that are both adaptive and provide probabilistic estimates of traversability metrics. In [29], a Gaussian process was proposed to build, and refine over various loops, a probabilistic energy map of a robot traversing an unknown terrain, while exploration was encouraged to converge to a minimum energy tour of the environment. However, this method is impractical for robots that explore new environments and do not perform repetitive loops. In [30], probabilistic slip models were learned for visually classified terrain types using Gaussian process regression. Then, a second Gaussian process leveraged spatial correlations in slip data for online slip model adaptation. However, this method still relied on the assumption of discretized terrain types and only considered the adaptation to small intraclass variations. Moreover, only the inclination of the terrain (i.e., pitch and roll) was considered as relevant geometric factor. Conversely, the Gaussian process is often computationally expensive and cannot scale to high-dimensional 3D geometric inputs, which are characteristic of highly unstructured environments. In [31], a meta-learning-based approach was proposed to adapt probabilistic predictions of two terramechanical parameters using neural networks and Bayesian linear regression. Then, a standard physics-based model [32] was adopted to link the two terramechanical parameters to the AMR dynamic. Hence, this method still suffered from the limitations of physics-based models mentioned above. Moreover, it only considers laterally symmetric motions in uniformly-sloped environments (i.e. the right and left wheels had identical motion and driving torques), while the interaction of more complex, unstructured, and non-uniform terrains was not considered.

### III. BACKGROUND ON META-CONV1D

In this paper, we exploit the Meta-Conv1D meta-learning framework and we extend it to consider probabilistic estimates. Meta-Conv1D has the advantage of end-to-end machine learning models in that no specific domain knowledge is required for their implementation while driving energy prediction and adaptation are entirely based on the collected data. Moreover, Meta-Conv1D enables the processing of high dimensional 3D geometric data, by means of Conv1D neural networks, thereby improving the prediction performance in highly unstructured, non-symmetric, environments.

In this section, related background information on the Meta-Conv1D methodology is provided.

#### A. CONV1D GEOMETRIC ANALYSIS

The terrain geometry is preprocessed using Conv1D neural networks. Conv1D analysis has reported remarkable capabilities to better capture complex wheel-terrain interactions

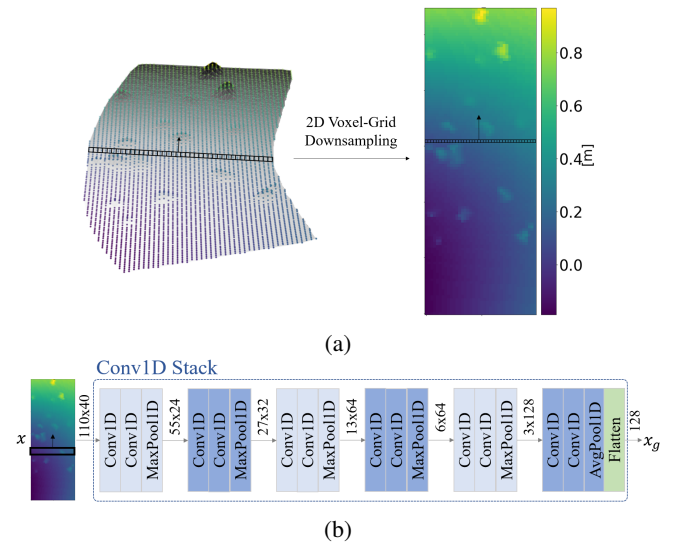


FIGURE 1: The Conv1D geometric analysis procedure. (a) The terrain point cloud, relative to the trajectory, is downsampled into a 2D-voxel grid. (b) The 2D-voxel grid is pre-processed by a stack of Conv1D neural networks to generate the latent geometric representation  $x_g$ .

over unstructured terrains, thereby leading to more accurate energy predictions in these scenarios [13] [15]. An illustration of the procedure is given in Fig 1. First, the terrain point cloud is downsampled into a 2D-voxel grid and rearranged such that each row can be seen as the terrain elevation under a section of the robot along its width at a specific time, while each column represents the time evolution of the terrain under that section as the robot advances along the trajectory (see Fig. 1a). Then, the 2D-voxel grid is fed to a Conv1D neural network which analyses the terrain geometry along the temporal axis and outputs the latent geometric representation  $x_g$  (see Fig. 1b). For brevity of the paper, the details are referred to [15]. In this paper, we set the voxel discretization, trajectory length, and the Conv1D architecture to be the same as in [15].

#### B. META-LEARNING

Meta-learning is concerned with learning algorithms that can efficiently adapt to new tasks. In line with [15], we exploit the meta-learning black-box approach that can be formally expressed as:

$$\theta^* = \underset{\theta}{\operatorname{argmin}} \mathbb{E}_{\mathcal{D}=\{\mathcal{D}^{tr}, \mathcal{D}^{ts}\} \sim \rho(\mathcal{D})} \sum_{j=1}^J [\mathcal{L}(f_\theta(x_j^{ts}, \mathcal{D}^{tr}), y_j^{ts})] \quad (1)$$

Where  $\rho(\mathcal{D})$  is a distribution over a collection of datasets  $\mathcal{D}$  from different tasks sharing some underlying similarity. Then, each dataset  $\mathcal{D}$  is divided into a meta-training dataset  $\mathcal{D}^{tr}$  and a meta-test dataset  $\mathcal{D}^{ts}$  both of them made of input-output pairs  $(x, y)$  from the same task. Then, the meta-learning objective is to find the parameters  $\theta$  of a function  $f_\theta$  such that, for all the tasks drawn from the distribution

$\rho$ , given  $K$  examples of a task  $\mathcal{D}^{tr} = \{(x, y)_{1:K}^{tr}\}$ , we can successfully predict new pairs from the same task on the meta-test dataset  $\mathcal{D}^{ts} = \{(x, y)_{1:J}^{ts}\}$ . In the black-box formulation,  $f_\theta$  is a single neural network trained in an end-to-end fashion to predict  $y_j^{ts}$  from  $x_j^{ts}$  and  $\mathcal{D}^{tr}$ . Therefore, the black-box formulation aims at modelling the predictive distribution:

$$p(y_j^{ts}|x_j^{ts}, \mathcal{D}^{tr}, \theta) = p(y_j^{ts}|x_j^{ts}, \{(x, y)_{1:K}^{tr}\}, \theta) \quad (2)$$

In our context, each task can be described as the problem of driving energy estimation  $y^{ts}$  of a terrain whose only available information  $x^{ts}$  is its geometry  $x_g$  (preprocessed with the method in Section III-A). Meanwhile, the terramechanical properties of the terrain are not explicitly given to the prediction model, while they are treated as the unknown characteristic that varies across tasks. Hence, a small number of local geometry-energy measurements  $\mathcal{D}^{tr}$  are exploited to implicitly retrieve the unknown terramechanical characteristics of the terrain and the information is leveraged to adapt the energy predictions accordingly. While in [15], single-point energy predictions were performed, in this paper, our goal is to explicitly model the probability distribution in Eq. (2) through neural network training.

#### IV. SOURCES OF UNCERTAINTY

In this section, we analyze the main factors responsible for uncertainties in the driving energy estimations and how they can affect the shape of the probability distribution in Eq. (2).

**1) Uncertainty of the geometric input data.** The geometry collection procedure in Section III-A, assumes that the robot initial position and speed are known and constant and that the on-board controller (see Section VI) can perfectly track the lateral position and longitudinal speed errors along the trajectory. While this is often the case in planar environments, unstructured geometries often pose a greater challenge to the onboard control system, thereby leading to the violation of these assumptions. As a consequence, the same terrain geometry  $x^{ts}$  can result in different values of energy consumptions  $y^{ts}$ . For example, depending on the lateral error of the robot, an obstacle present in a 2D-voxel grid may or may not be stepped over. Stepping over an obstacle often causes the variation of the wheel-ground contact area, possibly leading to unexpected slip, and altering the longitudinal speed and/or lateral error over the trajectory. Intuitively, these events (i.e., non-perfect tracking of the on-board controller and unexpected slip) often lead to increased energy costs compared to the nominal travel conditions (i.e., perfect tracking and no-slip). Therefore, we foresee that the uncertainty in prediction caused by these events can be expressed as a right-skewed probability distribution. This means that greater probabilities are associated with energy costs higher than the peak of the distribution (also called the mode).

**2) Uncertainty of the meta-training examples.** The meta-learning framework is an inherently uncertain procedure [33]. Indeed, few meta-training examples  $\mathcal{D}^{tr} = \{(x, y)_{1:K}^{tr}\}$  are

often insufficient to univocally retrieve the unknown terramechanical properties of a terrain. Moreover, some examples may be non-informative, i.e. they may carry little information about the properties of the traversed terrain. For example, a meta-training example consisting of a steep downhill trajectory that requires null energy consumption to be traversed (i.e. the robot always breaks) provides little information about the properties of that terrain as it may be equally representative of several terrain types. Furthermore, the meta-training examples can be ambiguous, as they are affected by the same uncertainty of the geometric input data described in point 1. Generally, more examples will help better recover the unknown characteristics of the terrain, thereby reducing the uncertainty of the energy estimation. Making *a priori* assumptions on the shape of the probability distribution caused by the meta-learning uncertainty is challenging. Intuitively, there is no apparent reason to expect skewed distributions due to this source of uncertainty.

Other common sources of uncertainty can be errors due to the precision of the instruments (e.g., measurement of energy consumption, point cloud collection, and robot localization). While those factors are likely present in real-world robots, they are strongly dependent on the specific sensors and algorithms adopted for the measurements. In this paper, we assume perfect knowledge of those data, as a detailed analysis of the uncertainty due to the instruments' errors is beyond the scope of this work. Despite this being a simplifying assumption, we note that our approach is entirely model and uncertainty agnostic, thereby allowing the direct integration of any other source of data uncertainty with minimal modifications to the proposed method.

#### V. METHODOLOGY

##### A. MODELLING UNCERTAINTY

In this paper, we choose to model the overall probability distribution of the energy estimates derived from all sources of uncertainty combined. Therefore, the most suitable probability distribution, which most accurately models the uncertainty in the driving energy prediction, must be identified. As discussed in Section IV, we foresee a right-skewed component in the resulting distribution. Moreover, another property of the driving energy consumption is that it is only defined for non-negative values (i.e.,  $y \geq 0$ ). As a consequence, the Gamma and Lognormal distributions are identified as the two most promising candidates [34]. The Gaussian and Gaussian mixture model (GMM) distributions are also considered, as they are the most common distributions, used in the majority of continuous problems [35]. Hence, we describe all the considered distribution models.

**1) Gamma Distribution** is a two-parameter family of continuous distributions. Its probability density function (PDF) can be defined as:

$$f(X, \alpha, \beta) = \begin{cases} \frac{X^{\alpha-1} e^{-\beta X} \beta^\alpha}{\Gamma(\alpha)} & X > 0 \\ 0 & X \leq 0 \end{cases} \quad (3)$$

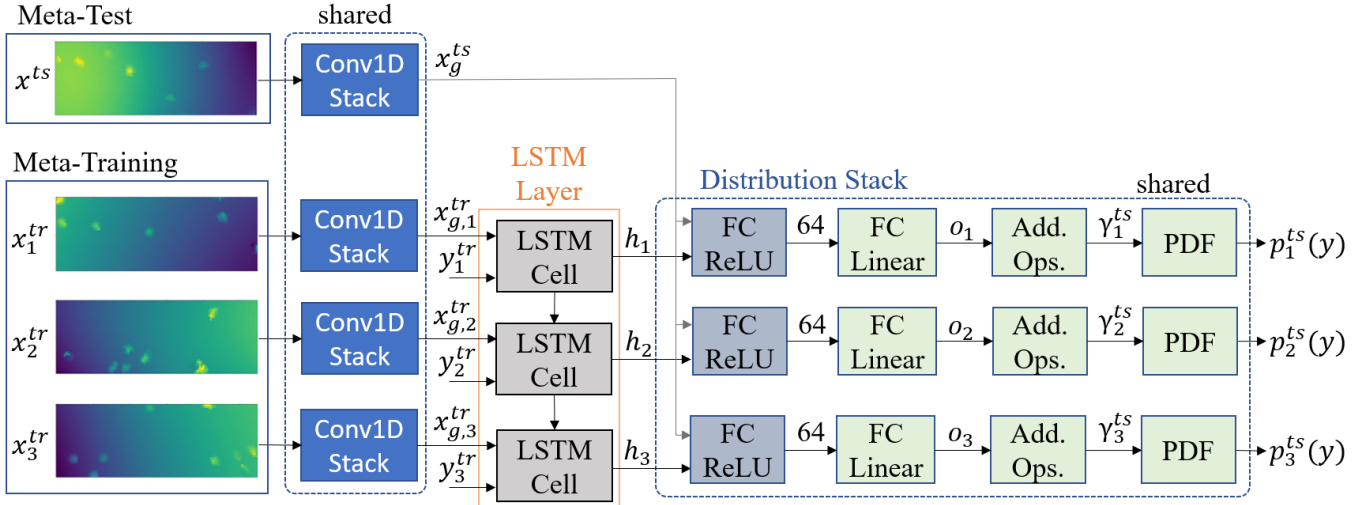


FIGURE 2: The probabilistic Meta-Conv1D neural network architecture. In light green, the parts that differ from [15] and that have different definitions for each of the four considered distribution models.

where  $X$  is a random variable (in our case, the driving energy consumption  $y$ ),  $\alpha, \beta > 0$  are respectively the shape and rate parameters, and  $\Gamma$  is the Gamma function  $\Gamma(\alpha) = \int_0^\infty x^{\alpha-1} e^{-x} dx$ . The Gamma distribution is right-skewed and defined only for real positive random variables. We also note that the mode of the Gamma distribution is not defined for  $\alpha \leq 1$ . Therefore, since in our application we are interested in the mode of the prediction, we only consider Gamma distributions with  $\alpha > 1$ .

**2) Lognormal Distribution** is a two-parameter family of continuous distributions where the logarithm of the random variable  $X$  is normally distributed. Its PDF can be defined as:

$$f(X, \mu, \sigma) = \begin{cases} \frac{1}{X\sigma\sqrt{2\pi}} \exp\left(-\frac{(\ln X - \mu)^2}{2\sigma^2}\right) & X > 0 \\ 0 & X \leq 0 \end{cases} \quad (4)$$

where  $\mu$  and  $\sigma$  are the mean and standard deviation of a random variable  $Y = \ln(X)$  that is normally distributed. Similar to the Gamma distribution, the Lognormal distribution is right-skewed and defined only for real positive random variables. We note that the mean and standard deviation of the Lognormal distribution are exponentially related to the  $\mu$  and  $\sigma$  parameters. For this reason, we heuristically set bounds on  $\mu$  and  $\sigma$  to avoid the explosion to infinitely high values of the Lognormal distribution. Specifically, in our application, we set  $\mu > -7$  and  $0 < \sigma < 1.6$ .

**3) Gaussian Distribution** is the standard, and most widely used, normal distribution, whose PDF can be defined as:

$$f(X, \mu, \sigma) = \frac{1}{\sigma\sqrt{2\pi}} \exp\left(-\frac{(X - \mu)^2}{2\sigma^2}\right) \quad (5)$$

where  $\mu$  and  $\sigma$  are the mean and standard deviation of the distribution. The Gaussian distribution is symmetric and defined for all real values. For this reason, we argue that the Gaussian distribution may be limiting to describe the driving energy prediction uncertainties in the context of mobile robots in

unstructured environments. We provide evidence of this in Section VII-A.

**4) Gaussian Mixture Model Distribution** is a weighted sum of  $M$  Gaussian components. Its PDF can be defined as:

$$f(X, w_{1:M}, \mu_{1:M}, \sigma_{1:M}) = \sum_{i=1}^M w_i \mathcal{N}(X, \mu_i, \sigma_i) \quad (6)$$

where  $w_{1:M}$  are the mixture weights (with  $\sum_{i=1}^M w_i = 1$ ), and each component  $\mathcal{N}(X, \mu_i, \sigma_i)$  is a Gaussian distribution as in Eq. (5). The advantage of GMM is that it is flexible, as it is not constrained to assume any specific shape while, by increasing the number of components  $M$ , it enables modeling of complex probability distributions or distributions with unknown shapes. However, the main downside is the increased complexity due to the higher number of parameters. Specifically, the number of parameters of a GMM is equal to  $3 \times M$ . In our experiments, we set  $M = 3$  as we experimentally observe minimal improvements in prediction for higher values of  $M$ . Moreover, as with the Gaussian distribution, the GMM is defined for both positive and negative real values, thereby being potentially limitative to describe the existing uncertainty in our problem. Finally, while the GMM is a valid approach if used exclusively for sampling, it does not provide analytical formulations of many useful probability metrics (e.g., mode, mean, CDF, PPF, etc.). Specifically, these metrics can only be approximated by assessing the PDF for several values of the random variable  $X$ . This makes the implementation of GMM more computationally expensive during inference than the other distribution models.

## B. NEURAL NETWORK ARCHITECTURE

In this paper, we propose four alternative versions of the probabilistic Meta-Conv1D neural network, one for each of the four distribution model described in Section V-A. Figure 2 shows the architecture of the proposed neural networks.

The network architecture is the same for all the methods, except for the parts in light green, which have different definitions for each of the four distribution models. The first part of the neural network (Conv1D stack, and LSTM layer) adopts the same architecture as the network in [15]. Specifically, the 2D-voxel grid geometries of the meta-training dataset  $x_{1:K}^{tr}$  (i.e. the previously traversed terrains) and of the meta-test dataset  $x_g^{ts}$  (i.e. the new terrain to analyze) are fed to multiple instances of the Conv1D stack (having shared weights) which process them and output the latent geometric representations  $x_{g,1:K}^{tr}$  and  $x_g^{ts}$ . Then,  $x_{g,1:K}^{tr}$  is concatenated to the respective driving energy consumptions  $y_{1:K}^{tr}$  (measured by the AMR while traversing the terrains). Hence, the resulting meta-training examples  $\mathcal{D}^{tr} = \{(x_g, y)_{1:K}^{tr}\}$  are fed to a Long-Short Term Memory (LSTM) layer with 128 units. In this way, each LSTM cell implicitly captures the unknown characteristics  $h_k$  of the terrain based on the  $k$  examples provided up until that point and passes on its current estimate to the next cell. In meta-learning, the maximum number of meta-training examples  $K$  is a heuristic application-dependent parameter. In line with [15], we experimentally set  $K = 3$ , as we observe minimal improvement in prediction error if more examples are provided. Then, the top part of the neural network (called Distribution stack) is a stack of one Fully Connected (FC) layer with 64 units and relu activation, followed by one FC layer with linear activation, Additional Operations (AddOps) layer, and PDF layer. The architecture of these last three layers varies depending on the distribution model considered. In this way, the Distribution stack (repeated  $K$  times with shared weights) takes as input the LSTM hidden vector  $h_k$  and the latent geometry of the meta-test terrain  $x_g^{ts}$ , and outputs the predicted probability distribution  $p_k^{ts}(y)$  given the  $k$  meta-training examples provided up to that point. Specifically, the AddOps layer takes the outputs  $o_k$  of the linear FC layer and generates the parameters of the probability distribution  $\gamma_k^{ts}$  (where  $\gamma$  stands for  $\alpha, \beta$  in case of the Gamma distribution,  $\mu, \sigma$  in case of the Lognormal distribution, etc.), while the PDF layer takes the  $\gamma_k^{ts}$  parameters and implements the PDF. The definition of the PDF for each distribution model was illustrated in Eqs. (3)-(6). In the following, we provide, for each method, the architecture of the linear FC layer and of the AddOps layer (note, the subscript  $k$ , relative to the meta-training example, is omitted for notation simplicity).

**1) Gamma Distribution:** the linear FC layer has 2 units, while the AddOps layer (that generates the  $\alpha$  and  $\beta$  parameters) is defined as:

$$\alpha = 1.001 + \text{SoftPlus}(o_1) \quad (7)$$

$$\beta = 1e - 3 + \text{SoftPlus}(o_2) \quad (8)$$

Where  $o_{1,2}$  are the two outputs of the FC layer and the  $\text{SoftPlus}$  operations ensure that  $\alpha > 1$  and  $\beta > 0$ .

---

**Algorithm 1** Probabilistic black-box meta-learning training procedure. In red, differences from [15].

---

**Input:** Collection of datasets  $\mathcal{D}$  from different terrain types  
**Input:** Distribution  $\rho$  over  $\mathcal{D}$   
**Input:** Mini-batch size N, number of examples K  
**Input:** Neural Network  $f_\theta$ , learning rate  $\alpha$

- 1: Randomly Initialize  $\theta$
- 2: **for** t=1,...,N **do**
- 3:     **for** j=1,...,N **do**
- 4:         Sample  $\mathcal{D}_j \sim \rho(\mathcal{D})$
- 5:         Randomly sample  $K$   $(x, y)^{tr} \sim \mathcal{D}_j$
- 6:         Randomly sample 1  $(x, y)^{ts} \sim \mathcal{D}_j$
- 7:          $p_{1:K}^{ts}(y) = f_\theta([(x, y)^{tr}_{1:K}, x^{ts}])$
- 8:     **end for**
- 9:      $\mathcal{L} = \frac{1}{NK} \sum_{j=1}^N \sum_{k=1}^K -\log p_{j,k}^{ts}(y = y_j^{ts})$
- 10:      $\theta \leftarrow \theta - \alpha \nabla_\theta \mathcal{L}$
- 11: **end for**

**Output:**  $\theta$

---

**2) Lognormal Distribution:** the linear FC layer has 2 units, while the AddOps layer (that generates the  $\mu$  and  $\sigma$  parameters) is defined as:

$$\mu = \text{ELU}(o_1, -7) \quad (9)$$

$$\sigma = 1e - 3 + (1.6 - 1e - 3) \times \text{Sigmoid}(o_2) \quad (10)$$

Where the  $\text{ELU}$  and  $\text{Sigmoid}$  operations ensure that  $\mu > -7$  and  $0 < \sigma < 1.6$ .

**3) Gaussian Distribution:** the linear FC layer has 2 units, while the AddOps layer (that generates the  $\mu$  and  $\sigma$  parameters) is defined as:

$$\mu = o_1 \quad (11)$$

$$\sigma = 1e - 3 + \text{SoftPlus}(o_2) \quad (12)$$

Where the  $\text{SoftPlus}$  operation ensures that  $\sigma > 0$ .

**4) Gaussian Mixture Model Distribution:** the linear FC layer has  $3 \times M$  units, while the AddOps layer (that generates the  $\mu_i$ ,  $\sigma_i$ , and  $w_i$  parameters, with  $i = 1 : M$ ) is defined as:

$$\mu_i = o_i \quad (13)$$

$$\sigma_i = 1e - 3 + \text{SoftPlus}(o_{M+i}) \quad (14)$$

$$w_i = \text{SoftMax}(o_{2M+i}, o_{(2M+1):3M}) \quad (15)$$

Where the  $\text{SoftPlus}$  operation ensures that  $\sigma_i > 0$  and the  $\text{SoftMax}$  operation ensures that  $\sum_{i=1}^M w_i = 1$ .

### C. TRAINING PROCEDURE

Algorithm 1 illustrates the training procedure for the proposed neural networks according to the probabilistic black-box meta-learning framework. At each training step, for each element in a mini-batch, we randomly select a dataset  $\mathcal{D}_j$ , from a collection of datasets each with different terramechanical properties. Then,  $K$  meta-training samples  $(x, y)^{tr}$

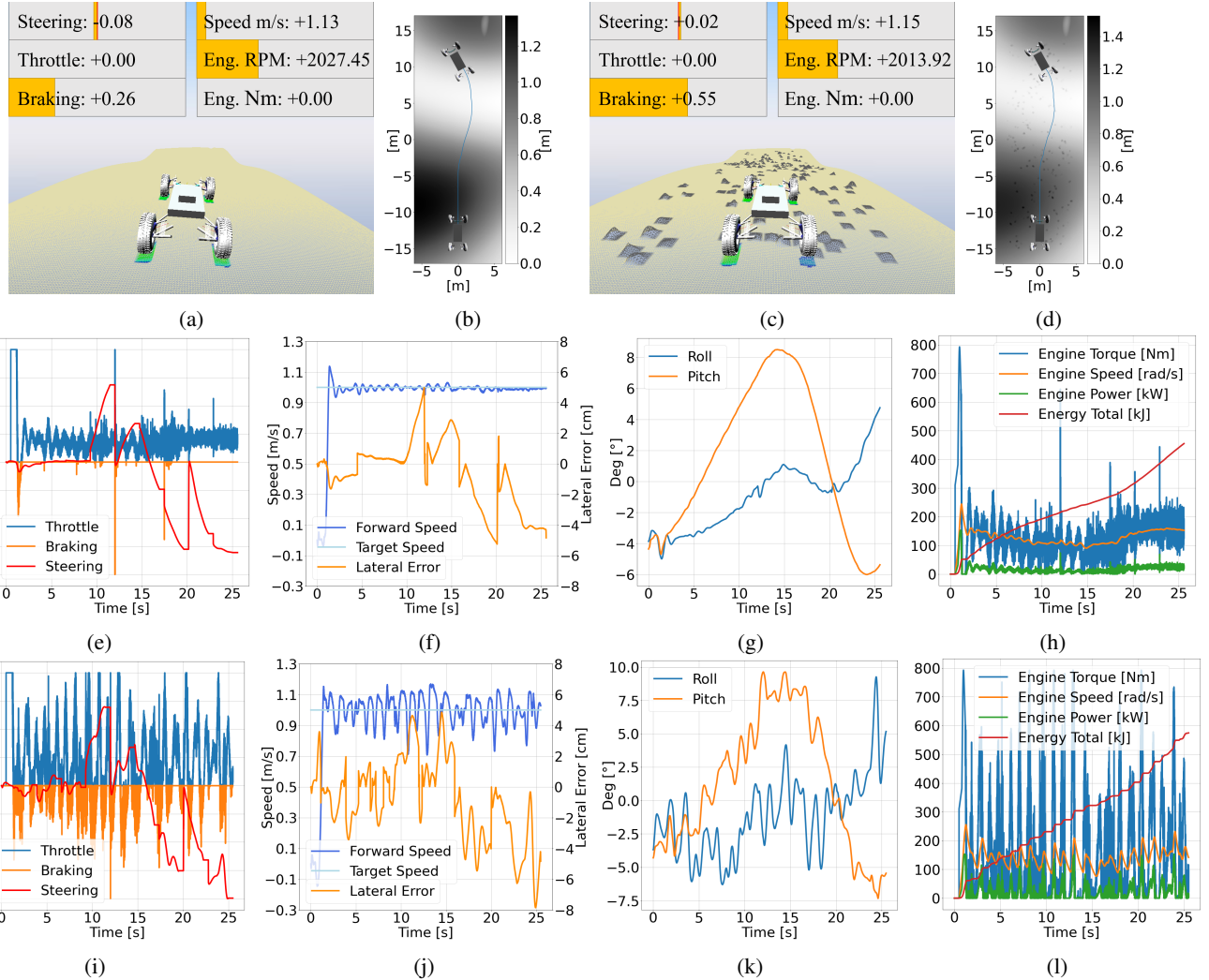


FIGURE 3: (a) Example of Simple environment with deformable terrain in the Chrono simulator. Colors on the wheel trace indicate the terrain sinkage depth after the AMR traversal. On the top left, the onboard controller commands to the AMR at that snapshot time. On the top right, monitored metrics of interest at that snapshot time (i.e., the AMR longitudinal speed, the engine round per minute, and the engine torque). (b) The DTM and the AMR traverse relative to the Simple environment. (c) Example of Unstructured environment, obtained by augmenting the DTM of the Simple environment with rigid, unstructured geometries (colored in black). (d) The DTM and AMR traverse relative to the Unstructured environment. From (e) to (h), the AMR state profiles along the traverse on the Simple environment and, from (i) to (l), on the Unstructured environment. From left (e/h) to right (h/l), the on-board controller commands (adimensional between  $[-1, 1]$ ), the controller tracking variables (i.e., the AMR longitudinal speed and lateral error), pitch and roll of the AMR, engine metrics of interest to the driving energy consumption.

and 1 meta-test sample  $(x, y)^{ts}$  are randomly sampled from  $\mathcal{D}_j$ . The predicted probability distributions  $p_{1:K}^{ts}(y)$  are obtained by feeding the samples to the network models as described in Section V-B. Hence, the loss for each batch is computed by averaging the negative log-likelihood (NLL) of the probability distributions evaluated on the true energy values  $y_j^{ts}$  (see Line 9). Finally, the network weights are updated to minimize the loss using stochastic gradient descent. In our experiments, each network is trained for 60 epochs, with mini-batch size  $N = 32$ , learning rate  $\alpha = 10^{-4}$ , and RMSprop optimizer [36].

#### D. ADAPTATION PROCEDURE

Upon training completion, new meta-training examples from the local terrain can be exploited to adapt the distribution model to the new terrain conditions. For instance, if one example is available, only the first LSTM cell must be fed with  $(x_g, y)_1^{tr}$ . Hence, the LSTM output  $h_1$  is used by the Distribution stack for the probabilistic energy prediction of new terrain geometries  $x^{ts}$ .

#### E. PATH PLANNING INTEGRATION

In this work, we adopt the same A\* lattice-space path planner developed in [15]. Particularly, the path planner adopts the

standard Meta-Conv1D approach to assign a single-point energy value to each edge of a state-lattice graph [37] and searches for an energy-optimal path using a heuristic A\* approach [38] [39]. For more information on the method refer to [15]. Meanwhile, the probabilistic models are not actively involved in the path planning procedure, while they are only integrated as additional layers to provide further probabilistic information about the already selected path solutions.

The implementation of more advanced probabilistic path planning methods may be the subject of future studies while, in this paper, we exclusively focus on the probabilistic reframing of the adaptive prediction model.

## VI. SIMULATOR AND DATA COLLECTION

The proposed method is tested using the dataset collected in [15]. The dataset is based on data gathered by an AMR navigating in several simulated unstructured scenarios using the Chrono dynamic simulator [40] and Soil Contact Model (SCM) [17]. SCM enables realistic modeling of arbitrary shaped wheel-terrain interactions in deformable terrains [41] [7] and retains a more efficient computing workload than alternative Finite Element or Discrete Element methods [18] [42]. In total, 17 terrain types are considered, which can be divided into 4 macro-categories: (1) high moisture content clays, (2) loose frictional, (3) compact frictional, and (4) dry clays. In addition, rigid, unstructured obstacles are embedded into half of the generated environments. Therefore, each dataset can be considered as made of three subsets: **Mixed** is the full dataset, (2) **Unstructured** is the subset that contains unstructured geometries, and (3) **Simple** is the subset that does not contain unstructured geometries.

The robot is driven over the generated environments at a constant speed of 1 m/s for a total of 1000 km (59 km for each of the 17 terrain types) [43]. The robot is subjected to a PID controller for the acceleration-brake pedals and a P controller for the wheel steering. Both controllers run at a frequency of 500 Hz. Hence, the geometry and driving energy data are collected during the traverses using simulated sensors, according to the method described in [15]. The final dataset is composed of 17 different datasets, each one from a different terrain type and made of 21 763 geometry-energy pairs (about 50 % Simple and 50 % Unstructured).

Fig. 3 illustrates an example of data collection in a Simple and Unstructured environment. In the example, the Unstructured scenario has the same terramechanical properties and Digital Terrain Model (DTM) as the Simple environment, but its DTM is randomly augmented with rigid, unstructured obstacles (see Figs. 3a and 3c). Hence, the same trajectory is commanded in both scenarios (see Figs. 3b and 3d). Figs. 3e-3g and Figs. 3i-3k show the AMR state profiles relative respectively to the Simple and Unstructured trajectories. As expected, greater efforts are required by the onboard controller to track the longitudinal speed and lateral error in the Unstructured scenario (note the higher acceleration, braking, and steering commands in Fig. 3i compared to Fig. 3e, and the higher tracking errors in Fig. 3j compared to

Fig. 3f). Indeed, stepping over the unstructured geometries causes external forces to act on the wheels and the constant variation of the wheel-ground contact area. For example, note the abrupt changes in the AMR pitch and roll orientations in Fig. 3k compared to the smoother variations in Fig. 3g. As a consequence, sharper peaks of motor power are required, in the unstructured scenario, in the attempt of tracking the target trajectory (see Fig. 3h and 3l). This illustrates how navigating over unstructured geometries majorly contributes to the increased uncertainty in the driving energy prediction and, thereby, provides insights into the potential benefits of a probabilistic formulation.

## VII. RESULTS

### A. VALIDATION PERFORMANCE

In this section, we compare the generalization performance of the proposed probabilistic models with the deterministic Meta-Conv1D approach. As in [15], we perform 5 test trials with different training-validation splits. For each trial, the training dataset is constituted by 4 randomly selected terrain types, and the corresponding datasets. Hence, the remaining 13 datasets are used for validation to assess the adaptation performance to new terrain types.

In Meta-Conv1D, the evaluation metrics of interest were the root mean squared error (RMSE) and the r<sup>2</sup> score (R<sup>2</sup>) between the predicted and true energy data, while no other information was available about the probability of the prediction. In the probabilistic models, the main evaluation metric is the NLL of the predicted distribution evaluated on the true energy data. Indeed, this metric is an indicator of the capability of the model to characterize the uncertainty in the prediction (the lower the NLL on the same dataset, the better the model). Moreover, we additionally monitor the RMSE and R<sup>2</sup> score between the mode (i.e. the peak) of the predicted distributions and the true energy data. In this way, we can compare the performance of the most-likely prediction in the deterministic and probabilistic cases.

Table 1 summarises the validation performance of the methods averaged over the 5 test trials. We observe that, as more meta-training examples are provided, the accuracy of the most-likely prediction improves for all the methods (RMSE decreases and R<sup>2</sup> increases) and the uncertainty is reduced for the probabilistic methods (NLL decreases). The decrease of NLL, in particular, provides evidence that more meta-training examples help better capture the unknown properties of the terrain, thereby resulting in lower prediction uncertainties. We observe that Meta-Conv1D has the best RMSE and R<sup>2</sup> score in all scenarios (except for the Simple subset with 3 meta-training examples, where Meta-Conv1D-Gaussian has marginally better performance). This can be explained by that, in Meta-Conv1D, the network is explicitly optimized to minimize the distance between the most-likely prediction and the true value. However, it can only provide a single-point energy estimate, while it cannot account for uncertainty considerations. Conversely, the probabilistic approaches are optimized to minimize the NLL. As

TABLE 1: The models' performance (averaged over 5 trials) for different numbers of meta-training examples (columns from 1 to 3) and different subsets of the validation dataset (Mixed, Unstructured, and Simple).

Meta-Training Examples	1			2			3		
	RMSE	R2	NLL	RMSE	R2	NLL	RMSE	R2	NLL
<b>Mixed</b>									
Meta-Conv1D [15]	<b>13.84</b>	<b>77.34</b>	-	<b>12.45</b>	<b>81.80</b>	-	<b>12.08</b>	<b>82.85</b>	-
Meta-Conv1D-Gamma	14.92	73.53	<b>1.324</b>	13.21	79.38	1.196	12.93	80.27	1.187
Meta-Conv1D-Lognorm	15.65	70.66	1.353	13.59	78.08	<b>1.172</b>	13.02	79.93	<b>1.117</b>
Meta-Conv1D-Gaussian	14.35	75.44	1.433	12.99	79.98	1.294	12.54	81.38	1.270
Meta-Conv1D-GMM	15.21	72.61	1.407	13.63	78.25	1.242	13.13	79.92	1.230
<b>Unstructured</b>									
Meta-Conv1D [15]	<b>16.38</b>	<b>68.27</b>	-	<b>15.00</b>	<b>73.48</b>	-	<b>14.52</b>	<b>75.10</b>	-
Meta-Conv1D-Gamma	17.75	62.63	1.623	15.87	70.18	1.517	15.50	71.51	1.505
Meta-Conv1D-Lognorm	18.70	58.35	<b>1.594</b>	16.65	67.10	<b>1.477</b>	16.02	69.55	<b>1.434</b>
Meta-Conv1D-Gaussian	17.12	65.17	1.717	15.82	70.30	1.615	15.28	72.31	1.588
Meta-Conv1D-GMM	17.89	62.18	1.659	16.41	68.34	1.544	15.86	70.49	1.508
<b>Simple</b>									
Meta-Conv1D [15]	<b>10.96</b>	<b>85.53</b>	-	<b>9.55</b>	<b>89.22</b>	-	9.31	89.70	-
Meta-Conv1D-Gamma	11.72	83.34	<b>1.017</b>	10.16	87.67	0.873	9.99	88.15	0.868
Meta-Conv1D-Lognorm	12.21	81.71	1.091	10.01	88.02	<b>0.843</b>	9.54	89.16	<b>0.781</b>
Meta-Conv1D-Gaussian	11.08	85.20	1.133	9.63	88.98	0.959	<b>9.31</b>	<b>89.73</b>	0.937
Meta-Conv1D-GMM	12.19	82.04	1.135	10.40	87.22	0.924	9.98	88.33	0.942

a consequence, the probabilistic models have the advantage of being capable to describe the existing uncertainty in the prediction, but at the cost of a degraded accuracy of the mode compared to Meta-Conv1D. This is particularly evident in the Unstructured subset, where the uncertainty of the data is higher. For example, the R2 score degradation of Meta-Conv1D-Gamma (M.C.-Gamma), Meta-Conv1D-Lognorm (M.C.-Lognorm), Meta-Conv1D-Gaussian (M.C.-Gaussian), and Meta-Conv1D-GMM (M.C.-GMM) with 3 meta-training example is of respectively [3.59 %, 5.55 %, 2.79 %, 4.61 %]. Meanwhile, the degradation in the Simple subset is more modest, being of respectively [1.55 %, 0.54 %, -0.03 %, 1.37 %]. M.C.-Gaussian has the lowest mode degradation overall. However, it also has considerably higher NNL in all scenarios. This confirms what was discussed in Section V-A, which is that, while the Gaussian distribution can provide most-likely predictions similar to the deterministic approach, it fails to correctly describe the uncertainty in the driving energy prediction. Meanwhile, M.C.-GMM has lower NLL than M.C.-Gaussian, but higher than M.C.-Gamma and M.C.-Lognorm. Moreover, M.C.-GMM presents the highest mode degradation (together with M.C.-Lognorm which has a similar mode degradation). The low overall performance of M.C.-GMM (both in terms of most-likely prediction and probability performance) can be explained by the higher number of parameters of this distribution, thereby making it more susceptible to over-fitting to the training dataset. Regarding M.C.-Lognorm, despite having a high mode degradation, it is the model with the lowest NLL overall (except for the Mixed and Simple subsets with 1 meta-training example, where M.C.-Gamma has the lowest NLL). Therefore, the Lognormal distribution is the most accurate model to describe the uncertainty in the prediction (especially in unstructured scenarios and if more than one meta-training

example is provided), but at the price of a higher error of the peak of the distribution. Finally, M.C.-Gamma provides the best overall compromise, being second-best in terms of mode degradation (after M.C.-Gaussian), and second-best in terms of uncertainty description (after M.C.-Lognorm).

An example of adaptation to a new terrain type and driving energy prediction according to the different methods is provided in Fig. 4. We observe that the first meta-training example ( $x, y$ )<sub>1<sup>tr</sup></sub> consists of a steep downhill trajectory that requires null driving energy consumption to be traversed. As discussed in Section IV, this represents a non-informative example as, based solely on this example, little information can be derived about the terramechanical properties of the terrain under analysis. As a consequence, Meta-Conv1D provides a single-point solution for the meta-test terrain that is affected by a large error. Moreover, Meta-Conv1D cannot provide any indication of the uncertainty of its estimation. Conversely, all the probabilistic approaches can describe the high uncertainty of the first prediction (i.e., flat distributions with large standard deviation). Hence, as more meta-training examples are provided, the models' most-likely predictions improve and the uncertainty of the probabilistic models decreases. This provides indications of the advantages of our approach that, by explicitly describing the uncertainty of the driving energy predictions, can provide more informed driving energy estimations. Furthermore, we observe that the first prediction of M.C.-GMM consists of a bimodal distribution. This provides further insights on that the first meta-training example is non-informative, as a well-defined single prediction, provided only that example, is challenging to identify. We note that M.C.-GMM is a flexible distribution unconstrained to any specific shape type. As more examples are provided, the second mode of M.C.-GMM is smoothed out and the PDF converges to a right-skewed distribution, similar to the M.C.-Gamma and

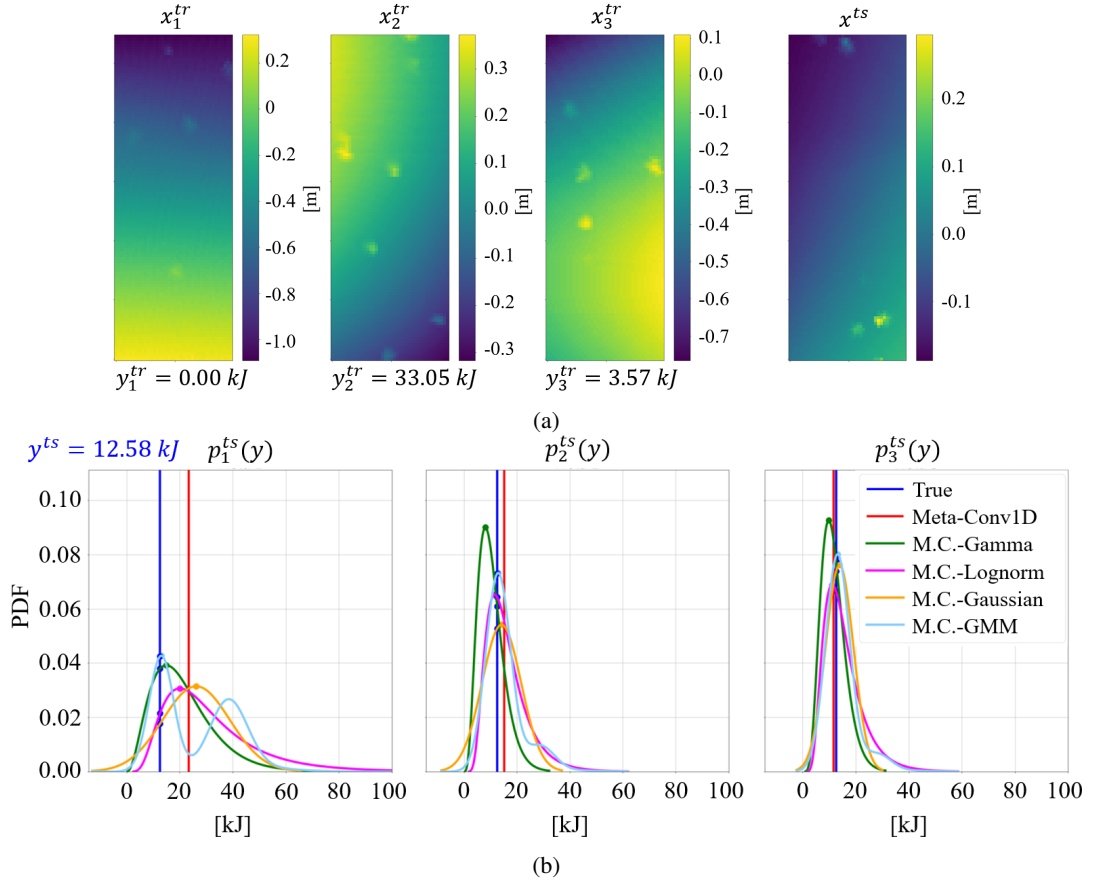


FIGURE 4: Example of terrain adaptation and driving energy prediction according to the different methods. (a) Three meta-training examples  $(x, y)_i^{tr}$  and one meta-test geometry  $x^{ts}$  are randomly selected from an unknown terrain type. (b) The ground truth (in blue) and predicted driving energy consumptions, relative to  $x^{ts}$ , are shown (single-point estimates or probability distributions depending on the model) after each new meta-training example is provided.

M.C.-Lognorm approaches. This provides evidence that a right-skewed distribution is well-suited for describing the prediction uncertainty in our problem. However, we observe that both M.C.-GMM and M.C.-Gaussian assign non-null probabilities to energy values lower than 0. Meanwhile, both M.C.-Gamma and M.C.-Lognorm are correctly defined only for positive energy values. Therefore, as the actual driving energy consumption is never negative, the latter two models can better describe the actual uncertainty in driving energy prediction. Finally, we observe that M.C.-Lognorm has often higher skewness and heavier tail than M.C.-Gamma. This can be interpreted as M.C.-Lognorm being a more conservative model, which tends to assign larger probabilities to energy values higher than the mode. The more conservative nature of M.C.-Lognorm may explain its overall better performance in terms of NLL, especially in the more complex Unstructured scenarios. However, this comes often at a price of overall higher degradation of the most-likely prediction compared to the less-skewed M.C.-Gamma approach.

In summary, if the most accurate most-likely prediction is required, without consideration of the prediction uncertainty, Meta-Conv1D is the most appropriate model. If the most

accurate modeling of the prediction uncertainty is desired, regardless of the mode accuracy, M.C.-Lognorm is the preferred option. Finally, if both accurate most-likely prediction and description of uncertainty are desired, M.C.-Gamma provides the best overall trade-off.

## B. PATH PLANNING INTEGRATION

In this section, we test the single-point and probabilistic energy estimators integrated into the A\* lattice-space path planner, as illustrated in Section V-E. Particularly, M.C.-Gaussian and M.C.-GMM are not considered, given their demonstrated inferior performance in the validation datasets. Hence, the prediction performance of the Meta-Conv1D, M.C.-Gamma, and M.C.-Lognorm methods are tested by conducting statistical analysis over 1080 random-start goal positions on randomly generated new scenarios with unstructured geometries and unforeseen terrain properties (selected from the 13 validation terrain types). Specifically, for each start-goal position: (1) the AMR navigates for 8.1 m and collects the three most recent geometry-energy pairs, (2) the three example pairs are used by Meta-Conv1D to plan a path to the next target, and (3) the prediction performance of the

three methods are compared on the selected path. To further increase the uncertainty of the terrain properties encountered during testing, random noise is added to each one of the 6 terramechanical parameters (with noise bounded to  $\pm 5\%$  of the value of each parameter). Hence, the number of unstructured geometries in the test environments is progressively increased after each 120 executions (from 0 to  $0.8 n_{ug}/m^2$ , where  $n_{ug}$  is the number of unstructured geometries). In this way, the impact of the unstructured geometries on the prediction performance of the three methods can be analyzed.

Fig. 5 summarises our findings. As with previous results, Meta-Conv1D retains the best most-likely prediction accuracy in all scenarios, having the highest R2 and lowest RMSE (see Fig. 5a). Meanwhile, M.C.-Lognorm experiences the largest mode degradation, while M.C.-Gamma has intermediate mode performance. Nevertheless, the most-likely prediction considerably degrades, for all the methods, as the number of unstructured geometries increases. For example, the R2 of Meta-Conv1D, M.C.-Gamma, and M.C.-Lognorm drops respectively from [92.57 %, 90.85 %, 91.21 %] with  $0 n_{ug}/m^2$  to [49.95 %, 47.61 %, 40.82 %] with  $0.8 n_{ug}/m^2$ . This provides further evidence of the large impact that unstructured geometries have on the complexity of the energy estimation. Therefore, the single-point Meta-Conv1D approach, despite its higher mode accuracy, may be limiting in highly unstructured scenarios, as it does not provide any additional information about the uncertainty of its estimations. Conversely, both M.C.-Gamma and M.C.-Lognorm can model the increasing uncertainty in the predictions. Fig. 5b illustrates the true total energy (sum of the 120 trajectories in each scenario) and the respective predictions according to the three methods. Specifically, for the probabilistic models, in addition to the mode, the 62 % and 98 % confidence of intervals (CIs) are shown. We observe that the mode predictions underestimate the true total energy values for all the methods. As previously mentioned, an excessive underestimation of driving energy can be dangerous in the context of AMRs navigating in challenging scenarios. Therefore, considerations about the existing prediction uncertainty can be beneficial. Hence, we observe that both the predicted uncertainties of M.C.-Gamma and M.C.-Lognorm increase and tend to be more right-skewed as the number of unstructured geometries increases. This provides evidence of that the uncertainty of the driving energy consumption, due to the presence of unstructured geometries, is skewed towards energy values higher than the mode. Particularly, M.C.-Lognorm presents increasingly larger skewness and heavier tail than M.C.-Gamma as the roughness of the environments rises. To further assess which of the two probabilistic models is better representative of the actual prediction uncertainty in our problem, Fig. 5c illustrates the percentage of true data points (in total,  $120 \times 3 = 360$  for each scenario) that falls within different predicted CIs according to the two methods. Specifically, the closer the resulting percentage is to the percentage of the respective CI, the more accurate is the predicted probability distribution. Hence, we observe

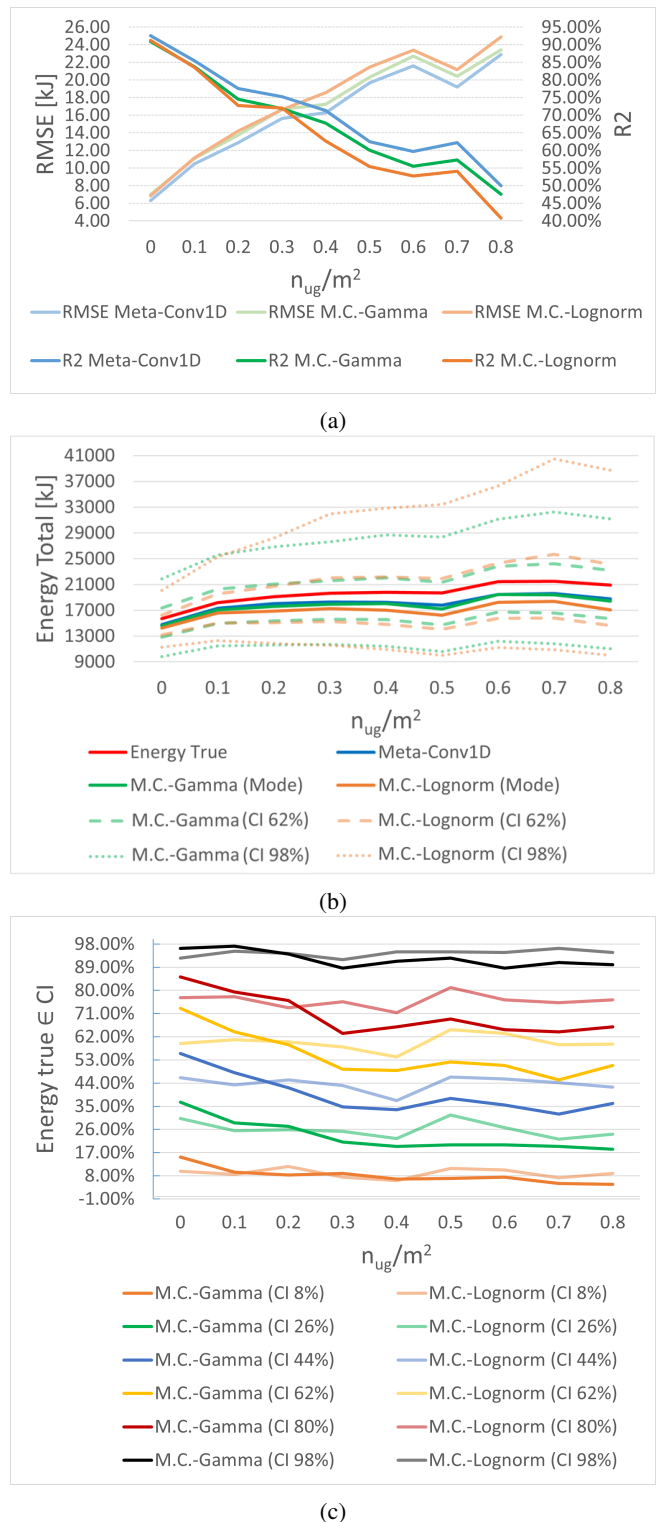


FIGURE 5: Effect of the number of unstructured geometries on the prediction performance for the deterministic and probabilistic approaches. (a) Prediction performance of the most-likely prediction. (b) Total energy (sum of 120 trajectories) true and predicted (mode, CI 62 %, and CI 98 %). (c) Percentage of true energy samples within different CIs.

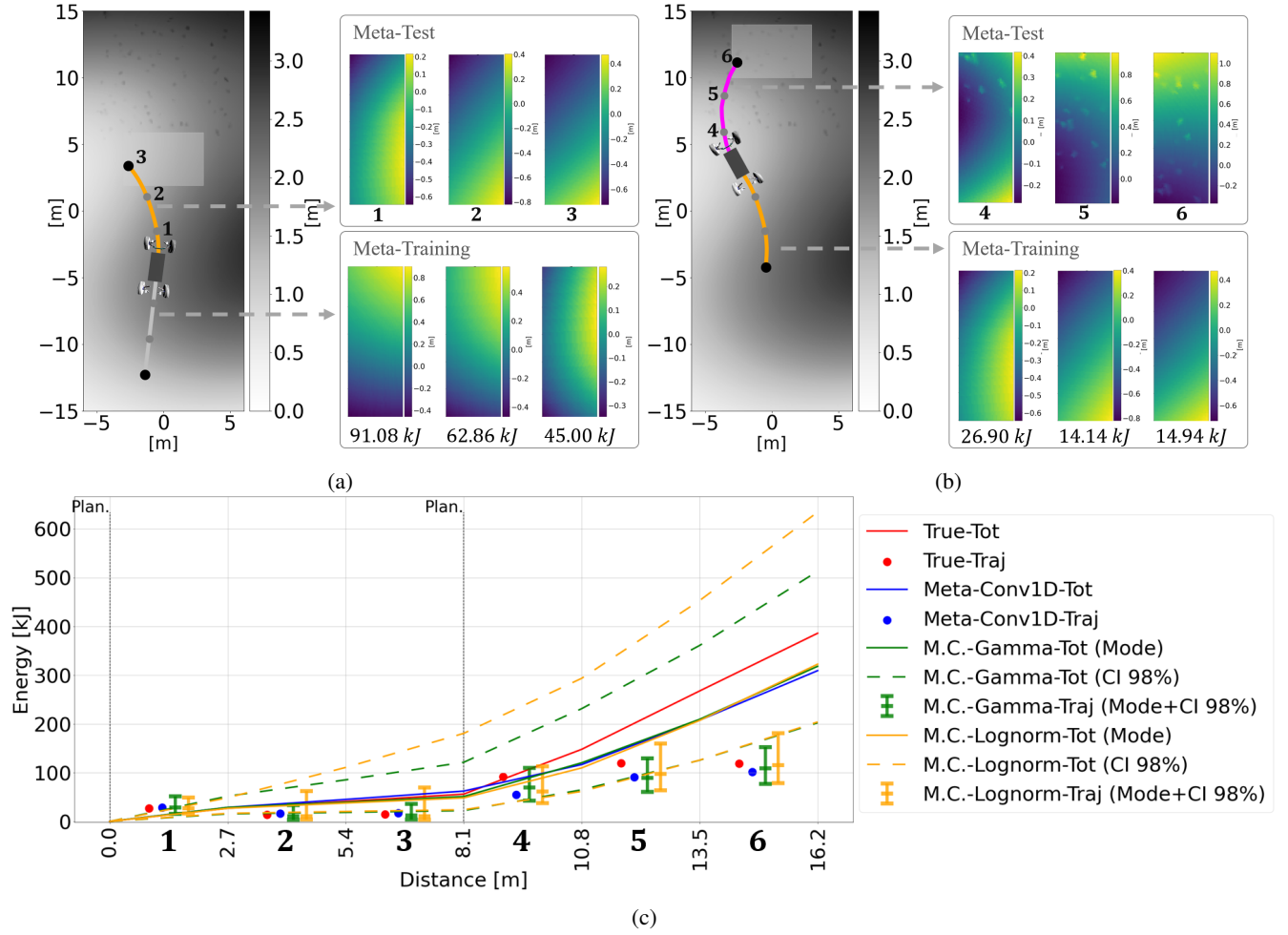


FIGURE 6: Example of two path planning procedures with probabilistic driving energy predictions. (a) The AMR plans the path 1-2-3 in an environment with  $0 \text{ } n_{ug}/\text{m}^2$ . (b) The AMR plans the path 4-5-6 in an environment with  $0.7 \text{ } n_{ug}/\text{m}^2$ . (c) The total (Tot) and the single trajectory (Traj) driving energy consumption (true and predicted according to the different models).

that M.C.-Lognorm shows superior overall performance than M.C.-Gamma. Indeed, the percentages of true data within the CIs of M.C.-Gamma are often larger than the expected values for  $n_{ug}/\text{m}^2 <= 0.2$  and considerably drop to lower values than the expected CIs for  $n_{ug}/\text{m}^2 >= 0.3$ . Meanwhile, the percentages of M.C.-Lognorm are approximately constant and closer to the expected values in all scenarios. This confirms that, despite the higher degradation in terms of mode accuracy of M.C.-Lognorm, its description of the prediction uncertainty is overall more accurate in both simple and unstructured environments.

Fig. 6 illustrates a qualitative example of the path planning procedure with probabilistic driving energy predictions. First, the AMR plans a path in an environment with  $0 \text{ } n_{ug}/\text{m}^2$  (see Fig. 6a). Then, it moves on a more challenging, unstructured scenario with  $0.7 \text{ } n_{ug}/\text{m}^2$  (see Fig. 6b). On the bottom right of both Figs. 6a and 6b, the recent experience from the previous trajectories (i.e., the 2D-voxel grid geometries and the respective driving energy consumptions) are used as meta-training examples to adapt the energy prediction models. On

the top right, the 2D-voxel grids of the next trajectories, of which the driving energy consumption must be determined (i.e., meta-test), are shown. As with previous results, the prediction accuracy of Meta-Conv1D considerably degrades as the roughness of the terrain increases (note, in Fig. 6c, the red and blue dots of the trajectory 4-5-6 compared to 1-2-3). Specifically, the true energy values of trajectory 4-5-6 are considerably higher than the Meta-Conv1D single-point predictions. Meanwhile, M.C.-Gamma and M.C.-Lognorm correctly capture the increased uncertainty of the second trajectory (note that the CI 98 % of both models increase and that the true energy values are appropriately contained within the CIs, for all the trajectories). As a consequence, while Meta-Conv1D provides a single value for the overall energy consumption that considerably underestimates the true energy cost, our proposed probabilistic framework provides more informative uncertainty boundaries, which can be crucial to the safety of AMRs in challenging, unstructured scenarios.

## VIII. CONCLUSION

In this study, we proposed a probabilistic deep-meta learning driving energy prediction model for AMRs navigating in complex, unstructured scenarios. Our work is based upon an existing deterministic meta-learning approach that is, in this paper, reframed to consider probabilistic estimates. We showed that, despite a marginal degradation of the most-likely prediction, our approach is more reliable than the deterministic method, as it can yield more informative uncertainty-aware estimations. Specifically, we remark the benefit of our approach to capture and explicitly model the uncertainty in the driving energy prediction caused by (1) insufficient and/or non-informative local measurements used to adapt the prediction model to the local terrain conditions and (2) the complex wheel-terrain interaction caused by traversing unstructured surfaces. Therefore, our method can be of interest to several applications of AMRs in unknown, challenging scenarios, for which an incorrect (e.g., overly optimistic) estimation of the driving energy consumption can compromise the safety and success of the mission.

This work can be extended in several directions. While in the current implementation all the sources of uncertainty were considered together, in a single prediction output, future works may investigate the development of more interpretable methods that explicitly distinguish among the different uncertainty components. Moreover, while the probabilistic prediction model was integrated, in this paper, into a deterministic path planner and only used as an additional information layer, future studies may investigate its active integration into more advanced probabilistic path planning frameworks (e.g., Monte Carlo Tree Search). Finally, while in this work our method was tested in simulation, exploiting the SCM 3D-body dynamic simulator, real-world tests will be required to further validate the results obtained during simulation.

## REFERENCES

- [1] J. Park, Y. L. Murphey, and M. Abul Masrur, “Intelligent energy management and optimization in a hybridized all-terrain vehicle with simple on-off control of the internal combustion engine,” *IEEE Transactions on Vehicular Technology*, vol. 65, no. 6, pp. 4584–4596, 2016.
- [2] O. Lamarre and J. Kelly, “Overcoming the challenges of solar rover autonomy: Enabling long-duration planetary navigation,” *CoRR*, vol. abs/1805.05451, 2018.
- [3] A. Dizqah, B. Ballard, M. Blundell, S. Kanarachos, and M. Innocente, “A non-convex control allocation strategy as energy-efficient torque distributors for on-road and off-road vehicles,” *Control Engineering Practice*, vol. 95, p. 104256, 2020. [Online]. Available: <https://www.sciencedirect.com/science/article/pii/S0967066118302879>
- [4] J. Y. Wong, *Theory of ground vehicles*. John Wiley & Sons, 2008.
- [5] M. Apfelbeck, S. Kuß, B. Rebele, and B. Schäfer, “A systematic approach to reliably characterize soils based on bevameter testing,” *Journal of Terramechanics*, vol. 48, no. 5, pp. 360–371, 2011.
- [6] A. Gallina, R. Krenn, M. Scharringhausen, T. Uhl, and B. Schäfer, “Parameter identification of a planetary rover wheel–soil contact model via a bayesian approach,” *Journal of Field Robotics*, vol. 31, no. 1, pp. 161–175, 2014.
- [7] A. Gallina, A. Gibbesch, R. Krenn, T. Uhl, and B. Schäfer, “Multibody simulation of planetary rover mobility in condition of uncertain soft terrain,” *Procedia IUTAM*, vol. 13, pp. 118–126, 2015.
- [8] J. B. Johnson, P. X. Duvoy, A. V. Kulchitsky, C. Creager, and J. Moore, “Analysis of mars exploration rover wheel mobility processes and the limitations of classical terramechanics models using discrete element method simulations,” *Journal of Terramechanics*, vol. 73, pp. 61–71, 2017.
- [9] N. Ganganath, C. Cheng, and C. K. Tse, “A constraint-aware heuristic path planner for finding energy-efficient paths on uneven terrains,” *IEEE Transactions on Industrial Informatics*, vol. 11, no. 3, pp. 601–611, 2015.
- [10] S. Fallah, B. Yue, O. Vahid-Araghi, and A. Khajepour, “Energy management of planetary rovers using a fast feature-based path planning and hardware-in-the-loop experiments,” *IEEE Transactions on Vehicular Technology*, vol. 62, no. 6, pp. 2389–2401, 2013.
- [11] G. Sakayori and G. Ishigami, “Energy efficient slope traversability planning for mobile robot in loose soil,” in *2017 IEEE International Conference on Mechatronics (ICM)*. IEEE, 2017, pp. 99–104.
- [12] V. Gruning, J. Pentzer, S. Brennan, and K. Reichard, “Energy-aware path planning for skid-steer robots operating on hilly terrain,” in *2020 American Control Conference (ACC)*, 2020, pp. 2094–2099.
- [13] M. Visca, A. Bouton, R. Powell, Y. Gao, and S. Fallah, “Conv1D energy-aware path planner for mobile robots in unstructured environments,” in *2021 IEEE International Conference on Robotics and Automation (ICRA)*, 2021, pp. 2279–2285.
- [14] M. Ono, T. J. Fuchs, A. Steffy, M. Maimone, and J. Yen, “Risk-aware planetary rover operation: Autonomous terrain classification and path planning,” in *2015 IEEE Aerospace Conference*, March 2015, pp. 1–10.
- [15] M. Visca, R. Powell, Y. Gao, and S. Fallah, “Meta-Conv1D energy-aware path planner for mobile robots in unstructured terrains,” *TechRxiv*, 2022. [Online]. Available: <https://doi.org/10.36227/techrxiv.19538575.v1>
- [16] F. Zhou, R. E. Arvidson, K. Bennett, B. Trease, R. Lindemann, P. Bellutta, K. Iagnemma, and C. Senatore, “Simulations of mars rover traverses,” *Journal of Field Robotics*, vol. 31, no. 1, pp. 141–160, 2014.
- [17] F. Buse, R. Lichtenheldt, and R. Krenn, “Scm-a novel approach for soil deformation in a modular soil contact model for multibody simulation,” *IMSD2016 e-Proceedings*, 2016.
- [18] R. He, C. Sandu, A. K. Khan, A. G. Guthrie, P. S. Els, and H. A. Hamersma, “Review of terramechanics models and their applicability to real-time applications,” *Journal of Terramechanics*, vol. 81, pp. 3–22, 2019.
- [19] B. Rothrock, R. Kennedy, C. Cunningham, J. Papon, M. Heverly, and M. Ono, “Spoc: Deep learning-based terrain classification for mars rover missions,” in *AIAA SPACE 2016*, 2016, p. 5539.
- [20] R. González and K. Iagnemma, “Deepterramechanics: Terrain classification and slip estimation for ground robots via deep learning,” *CoRR*, vol. abs/1806.07379, 2018. [Online]. Available: <http://arxiv.org/abs/1806.07379>
- [21] A. Shaukat, P. C. Blacker, C. Spiteri, and Y. Gao, “Towards camera-lidar fusion-based terrain modelling for planetary surfaces: Review and analysis,” *Sensors*, vol. 16, no. 11, 2016. [Online]. Available: <https://www.mdpi.com/1424-8220/16/11/1952>
- [22] G. Huang, X. Yuan, K. Shi, Z. Liu, and X. Wu, “A 3-d multi-object path planning method for electric vehicle considering the energy consumption and distance,” *IEEE Transactions on Intelligent Transportation Systems*, pp. 1–13, 2021.
- [23] S. Higa, Y. Iwashita, K. Otsu, M. Ono, O. Lamarre, A. Didier, and M. Hoffmann, “Vision-based estimation of driving energy for planetary rovers using deep learning and terramechanics,” *IEEE Robotics and Automation Letters*, vol. 4, no. 4, pp. 3876–3883, 2019.
- [24] H. Peng, “A comprehensive overview and survey of recent advances in meta-learning,” *ArXiv*, vol. abs/2004.11149, 2020.
- [25] X. Song, Y. Yang, K. Choromanski, K. Caluwaerts, W. Gao, C. Finn, and J. Tan, “Rapidly adaptable legged robots via evolutionary meta-learning,” *2020 IEEE/RSJ International Conference on Intelligent Robots and Systems (IROS)*, pp. 3769–3776, 2020.
- [26] R. Kaushik, T. Anne, and J.-B. Mouret, “Fast online adaptation in robotics through meta-learning embeddings of simulated priors,” *2020 IEEE/RSJ International Conference on Intelligent Robots and Systems (IROS)*, pp. 5269–5276, 2020.
- [27] A. Nagabandi, I. Clavera, S. Liu, R. S. Fearing, P. Abbeel, S. Levine, and C. Finn, “Learning to adapt in dynamic, real-world environments through meta-reinforcement learning,” *arXiv: Learning*, 2019.
- [28] M. Visca, R. Powell, Y. Gao, and S. Fallah, “Deep meta-learning energy-aware path planner for unmanned ground vehicles in unknown terrains,” *IEEE Access*, vol. 10, pp. 30 055–30 068, 2022.
- [29] S. Martin and P. Corke, “Long-term exploration tours for energy constrained robots with online proprioceptive traversability estimation,” in *2014 IEEE International Conference on Robotics and Automation (ICRA)*, 2014, pp. 5778–5785.

- [30] C. Cunningham, M. Ono, I. Nesnas, J. Yen, and W. L. Whittaker, "Locally-adaptive slip prediction for planetary rovers using gaussian processes," in *2017 IEEE International Conference on Robotics and Automation (ICRA)*, 2017, pp. 5487–5494.
- [31] S. Banerjee, J. Harrison, P. M. Furlong, and M. Pavone, "Adaptive meta-learning for identification of rover-terrain dynamics," *ArXiv*, vol. abs/2009.10191, 2020.
- [32] K. Iagnemma, S. Kang, H. Shibly, and S. Dubowsky, "Online terrain parameter estimation for wheeled mobile robots with application to planetary rovers," *IEEE Transactions on Robotics*, vol. 20, no. 5, pp. 921–927, 2004.
- [33] C. Finn, K. Xu, and S. Levine, "Probabilistic model-agnostic meta-learning," in *Proceedings of the 32nd International Conference on Neural Information Processing Systems*, ser. NIPS'18. Red Hook, NY, USA: Curran Associates Inc., 2018, p. 9537–9548.
- [34] N. L. Johnson, S. Kotz, and N. Balakrishnan, *Continuous univariate distributions. Vol. 1*, 2nd ed., ser. Wiley Series in Probability and Mathematical Statistics: Applied Probability and Statistics. John Wiley & Sons, Inc., New York, 1994, a Wiley-Interscience Publication.
- [35] D. A. Reynolds, "Gaussian mixture models." *Encyclopedia of biometrics*, vol. 741, no. 659–663, 2009.
- [36] T. Tieleman and G. Hinton, "Lecture 6.5—RmsProp: Divide the gradient by a running average of its recent magnitude," COURSERA: Neural Networks for Machine Learning, 2012.
- [37] M. Pivtoraiko, R. A. Knepper, and A. Kelly, "Differentially constrained mobile robot motion planning in state lattices," *Journal of Field Robotics*, vol. 26, no. 3, pp. 308–333, 2009.
- [38] P. E. Hart, N. J. Nilsson, and B. Raphael, "A formal basis for the heuristic determination of minimum cost paths," *IEEE Transactions on Systems Science and Cybernetics*, vol. 4, no. 2, pp. 100–107, July 1968.
- [39] R. Dechter and J. Pearl, "Generalized best-first search strategies and the optimality of A\*," *J. ACM*, vol. 32, no. 3, p. 505–536, Jul. 1985. [Online]. Available: <https://doi.org/10.1145/3828.3830>
- [40] A. Tasora, R. Serban, H. Mazhar, A. Pazouki, D. Melanz, J. Fleischmann, M. Taylor, H. Sugiyama, and D. Negruț, "Chrono: An open source multi-physics dynamics engine," in *International Conference on High Performance Computing in Science and Engineering*. Springer, 2015, pp. 19–49.
- [41] J. Dallas, K. Jain, Z. Dong, L. Sapronov, M. P. Cole, P. Jayakumar, and T. Ersal, "Online terrain estimation for autonomous vehicles on deformable terrains," *Journal of Terramechanics*, vol. 91, pp. 11–22, 2020.
- [42] S. Taheri, C. Sandu, S. Taheri, E. Pinto, and D. Gorsich, "A technical survey on terramechanics models for tire–terrain interaction used in modeling and simulation of wheeled vehicles," *Journal of Terramechanics*, vol. 57, pp. 1–22, 2015.
- [43] M. Visca, S. Kuutti, R. Powell, Y. Gao, and S. Fallah, "Deep learning traversability estimator for mobile robots in unstructured environments," in *Towards Autonomous Robotic Systems*. Cham: Springer International Publishing, 2021, pp. 203–213.



MARCO VISCA received the B.Sc. in Aerospace Engineering and the M.Sc. in Mechatronic Engineering from the Politecnico di Torino, Italy, in 2016 and 2018, respectively. He is currently pursuing the Ph.D. degree in Robotics with the University of Surrey, Guildford, U.K.

His research interests include artificial intelligence, machine learning, and their application to autonomous vehicles and robots in challenging environments.



**ROGER POWELL** is head of the Robotics and AI Group within the Cybernetics Department of RACE (Remote Applications in Challenging Environments), which is part of the UK Atomic Energy Authority (UKAEA). Prior to this appointment he was a Senior Lecturer at Brunel University, in the department of Electronic and Computer Engineering.



**YANG GAO** (S'00-M'03-SM'09) received the B.Eng. degree in electrical and electronics engineering and the Ph.D. degree in artificial intelligence, control and instrumentation from Nanyang Technological University (NTU), Singapore, in 2000 and 2003, respectively. She is the Professor of Space Autonomous Systems and Founding Head of the multi-award winning STAR LAB at the Surrey Space Centre, University of Surrey, Guildford, UK. She specializes in robotic vision, machine learning, and biomimetic mechanism for industrial applications in extreme environments. She brings over 20 years of R&D experience in solving robotic system problems, and is actively involved in development of real-world space missions, such as ESA's ExoMars, Proba3 and Lunar VMMO, UK's MoonLITE and Moonraker, and CNSA's Chang'E3.



**SABER FALLAH** is the Director of the Connected Autonomous Vehicles Lab (CAV-Lab) at the Department of Mechanical Engineering Sciences at the University of Surrey, where he leads several research activities funded by the UK and European governments (e.g. EPSRC, Innovate UK, H2020, KTP) in collaboration with major companies active in autonomous vehicle and robot technologies. CAV-Lab provides a unique laboratory to design, develop and test the next generation of robotics and autonomous systems used for remote assembly and manufacture, highly automated transportation systems and missions in hazardous environments including space. CAV-Lab also provides expertise in distributed control systems, AI and machine learning, and predictive optimisation techniques. Prior to joining the University of Surrey, he was part of a cross-disciplinary team in Green Intelligent Transportation Systems research (University of Waterloo, Canada). His research interests include deep reinforcement learning, advanced control and prediction and their application to autonomous robot systems.